Protective effect of curcumin against irinotecan-induced intestinal mucosal injury via attenuation of NF-κB activation, oxidative stress and endoplasmic reticulum stress

MANZHAO OUYANG[1*], ZHENTAO LUO[1*], WEIJIE ZHANG[1*],
DAJIAN ZHU[2], YAN LU[1], JINHAO WU[1] and XUEQING YAO[3,4]

[1]Department of Gastrointestinal Surgery, Shunde Hospital, Southern Medical University,
Shunde, Foshan, Guangdong 528308; [2]Department of Gastrointestinal Surgery,
Shunde Women and Children's Health Care Hospital of Shunde, Foshan,
Guangdong 528300; [3]Department of General Surgery, Guangdong General Hospital and
Guangdong Academy of Medical Sciences; [4]The Second School of Clinical Medicine,
Southern Medical University, Guangzhou, Guangdong 510080, P.R. China

Abstract. Irinotecan (CPT-11) is a DNA topoisomerase I inhibitor which is widely used in clinical chemotherapy, particularly for colorectal cancer treatment. However, late-onset diarrhea is one of the severe side-effects of this drug and this restricts its clinical application. The present study aimed to investigate the protective effects of curcumin treatment on CPT-11-induced intestinal mucosal injury both *in vitro* and *in vivo* and to elucidate the related mechanisms involved in these effects. For this purpose, mice were intraperitoneally injected with CPT-11 (75 mg/kg) for 4 days to establish a model of late-onset diarrhea. Curcumin (100 mg/kg) was intragastrically administered 8 days before the injection of CPT-11. Injury to small intestinal tissues was examined by H&E staining. The protein expression of prolyl 4-hydroxylase subunit beta (P4HB) and peroxiredoxin 4 (PRDX4) was detected by immunohistochemistry, as well as western blot analysis. IEC-6 cell viability was detected by MTT assay. Flow cytometry was performed to examine the cell apoptotic rate, mitochondrial membrane potential and reactive oxygen species (ROS) generation. Immunofluorescence was used to observe the localization of nuclear factor (NF)-κB. The levels of cleaved caspase-3, glucose-regulated protein, 78 kDa (GRP78), P4HB, PRDX4 and CHOP were detected by western blot analysis. The results revealed that *in vivo*, curcumin effectively attenuated the symptoms of diarrhea and abnormal intestinal mucosa structure induced by CPT-11 in nude mice. Treatment with curcumin also increased the expression of P4HB and PRDX4 in the tissue of the small intestine. *In vitro*, curcumin, exhibited little cytotoxicity when used at concentrations <2.5 µg/ml for 24 h in IEC-6 cells. At this concentration, curcumin also improved cell morphology, inhibited apoptosis, maintained mitochondrial membrane potential and reduced the elevated levels of ROS induced by CPT-11 (20 µg/ml). Furthermore, curcumin abolished NF-κB signal transduction and protected the cells from CPT-11-induced apoptosis by upregulating the expression of molecular chaperones, such as GRP78, P4HB and PRDX4, and suppressing the levels of the apoptosis-related proteins, CHOP and cleaved caspase-3. On the whole, our data indicate that curcumin exerted protective effects against CPT-11-induced intestinal mucosa injury. The protective effects of curcumin are mediated by inhibiting the activation of NF-κB, and suppressing oxidative stress and endoplasmic reticulum stress.

Introduction

Irinotecan (CPT-11), a semi-synthetic camptothecin topoisomerase I inhibitor, is mainly used in the treatment of patients with advanced colorectal cancer (1). However, CPT-11-induced intestinal mucosal injury, such as late-onset diarrhea, has significantly impeded cancer chemotherapy treatment. The overall incidence of clinically significant diarrhea due to CPT-11 treatment is up to 87%, with the incidence of grade 3 or 4 diarrhea ranging between 30-40% (2). With the long duration or the improper treatment of diarrhea, patients may develop excessive dehydration, electrolyte loss, acid-base balance disorders, shock and even death (3).

The pathogenesis of CPT-11-induced intestinal mucosal injury is complex. It is generally accepted that CPT-11 and its active metabolite, SN-38, can damage intestinal mucosal

Correspondence to: Professor Xueqing Yao, Department of General Surgery, Guangdong General Hospital and Guangdong Academy of Medical Sciences, 106 Zhongshan 2nd Road, Guangzhou, Guangdong 510080, P.R. China
E-mail: yjb9211@21cn.com

*Contributed equally

cells directly (4). Moreover, CPT-11 can activate a variety of signaling pathways, such as the nuclear factor (NF)-κB pathway, increase the expression of inflammation-related factors, such as cyclooxygenase-2 (COX-2) and prostaglandin E_2 (PGE2) and promote the levels of the inflammatory factors, tumor necrosis factor (TNF)-α and interleukin (IL)-1β in succession, which eventually leads to intestinal inflammation-related damage (5). In addition, polymorphisms in the *UGT1A1* gene (6) the expression of tight junction proteins (7) and bacterial translocation (8) are the probable mechanisms responsible for CPT-11-induced intestinal mucosal injury.

Curcumin is a polyphenolic compound derived from dried turmeric rhizome of a plant in the ginger family. A number of experimental studies have demonstrated that curcumin exerts anti-inflammatory, antioxidant and anti-tumor effects (9-11). According to a previous study, curcumin was shown to protect intestinal mucosal barrier function in MTX-induced enteritis in rat by suppressing NF-κB activation and inhibiting the activation of p38 mitogen-activated protein kinase (MAPK) (12). Similarly, Arafa *et al* (13) suggested that curcumin exerted protective effects against ulcerative colitis induced by dextran sulfate sodium (DSS) in rats by downregulating malondialdehyde (MDA), and upregulating superoxide dismutase (SOD), glutathione-S-transferase (GST) and GSH. In addition, our previous study also demonstrated that curcumin enhanced the CPT-11-induced apoptosis of LoVo colorectal cancer cells. We then selected 5 proteins of interest [glutathione S-transferase Mu 5 ($GSTM_5$), peroxiredoxin 4 (PRDX4), prolyl 4-hydroxylase subunit beta (P4HB), calpain small subunit 1 (CAPNS1) and signal sequence receptor subunit 4 (SSR4)] out of 54 differential expressed proteins identified by mass spectroscopy. P4HB and PRDX4 are oxidative stress- and endoplasmic reticulum (ER) stress-related proteins, respectively (14). We suspected that these two proteins may be involved in the protective effects of curcumin on CPT-11-induced intestinal mucosal injury.

The current study aimed to investigate the protective effects of curcumin on CPT-11-induced intestinal mucosal injury and to elucidate the associated mechanisms via *in vivo* and *in vitro* experimentation.

Materials and methods

Chemicals. Curcumin, dimethylsulfoxide (DMSO), 3-(4,5-dimethylthiazol-2-yl)-2,5-diphenyltetrazolium bromide (MTT) and sodium carboxymethyl cellulose (CMC-Na) were purchased from Sigma-Aldrich (St. Louis, MO, USA). Curcumin was purchased from Sigma-Aldrich [assay≥98% (HPLC)] and dissolved in DMSO at a concentration of 40 mg/ml, preserved at -80˚C and protected from light. Irinotecan (CPT-11) was purchased from Hengrui Medicine Co. Ltd. (Jiangsu, China). SOD and MDA were purchased from Jiancheng Biotech Ltd. (Nanjing, China). The Annexin-V-FITC apoptosis detection kit was obtained from KeyGen (Nanjin, China). Finally, the JC-1 mitochondrial membrane potential assay kit was purchased from the Beyotime Institute of Biotechnology (Nantong, China).

Animals. Eighteen BALB/c nude mice (6 weeks old, male, weighing 18±2 g) were purchased from Sun Yat-sen University

Animal Center Inc. (Guangzhou, China) and raised in a SPF environment. The Laboratory Animal Use Certificate number for these animals is SCXK(YUE)2011-0029. All the mice were housed in a clean laminar flow rack in the SPF environment with a constant temperature (20-26˚C) and constant humidity (50-56%) and were exposed to a 12-h light/dark cycle, and allowed free access to standard laboratory sterile food and water. The cages, bedding materials, food and drinking water of the nude mice were sterilized by high-pressure steam and replaced timely under aseptic conditions. The 18 BALB/c-nu mice were randomly assigned to 3 groups as follows: The normal control group (CON), the diarrhea model group (CPT-11) and curcumin therapy group (CPT-11 + CUR) (n=6 mice per group). Mice were intraperitoneally injected with CPT-11 (75 mg/kg) for 4 days to establish a model of late-onset diarrhea. Mice in the curcumin therapeutic group were intraperitoneally injected with CPT-11 (75 mg/kg) for 4 days, and treated with curcumin (100 mg/kg) by intragastric administration for 8 days at the same time. Mice in the normal control group and diarrhea model group received the vehicle only (0.5% CMC-Na). This study was approved by the Institutional Animal Care and Use Committee of Southern Medical University (Foshan, China).

Histological examination. The animals were sacrificed by cervical dislocation on the 9th day. Intestinal samples obtained and fixed in 4% paraformaldehyde for 24 h. After rinsing with running water, the samples were dehydrated with an increasing ethanol series, washed in xylene and embedded in paraffin. Paraffin blocks were cut 4-μm-thick, deparaffinized in xylene and hydrated using an serial dilution of ethanol. The intestinal tissue sections were stained with hematoxylin and eosin (H&E) solution (Solarbio Science & Technology Co., Ltd., Beijing, China) and observed with an optical microscope (Olympus Corp., Tokyo, Japan).

Immunohistochemical analysis. The tissue sections were conventionally dewaxed in water and then blocked with 1% BSA for 30 min at room temperature. The sections were incubated with primary antibodies to P4HB (1:100; cat. no. ab2792; Abcam, Cambridge, MA, USA) and PRDX4 (1:100; cat. no. BS6787; BioWorld, Visalia, CA, USA) in a wet box at 4˚C overnight. The sections were subsequently incubated with biotinylated goat anti-rabbit IgG for 30 min and avidin-biotin-peroxidase complex (cat. no. SP-9000; Biotin-Streptavidin HRP Detection Systems; ZSGB-BIO, Beijing, China) for a further 30 min. The sections were then stained with DAB solution. After counterstaining with hematoxylin, the sections were dehydrated, cleared, mounted and examined under a microscope. Images (x400 magnification) were then captured using a light microscope (Olympus BX41-32P02-FLB3; Olympus Corp.). Using Image-Pro Plus 6 software to analyze, the average optical density values obtained (IOD) represents the expression level of the proteins.

Cells and cell culture conditions. The normal rat small intestine epithelial cell line, IEC-6, was obtained from the American Type Culture Collection (ATCC, Manassas, VA, USA). This cell line was cultured in DMEM (Gibco/Thermo Fisher Scientific,

Waltham, MA, USA) with 1% penicillin-streptomycin and 10% fetal bovine serum (Gibco/Thermo Fisher Scientific) in a humidified 5% CO_2 atmosphere at 37˚C.

Evaluation of cell viability via MTT assay. To investigate the viability of the IEC-6 cells treated with curcumin or CPT-11, the cells were seeded in 96-well plates at a density of 1×10^5/ml in 100 μl of medium. The cells were then exposed to various concentrations of curcumin (0.6, 1.2, 2.5, 5, 10, 20 and 40 μg/ml) or CPT-11 (2.5, 5, 10, 20, 40, 50, 80 and 100 μg/ml) for 24 h. The medium was then removed and MTT solution (5 mg/ml) was added to the cells at 150 μl in each well, followed by incubation for a further 4 h at 37˚C. The MTT solution was removed after 4 h and 150 μl of DMSO were added to each well for 10 min in the dark. The absorbance was then measured at 490 nm on a microplate reader (MD SpectraMax M5; Molecular Devices, LLC., San Jose, CA, USA).

To investigate the protective effects of curcumin on CPT-11-induced damage to IEC-6 cells, the cells were co-treated with curcumin (0.6, 1.2 and 2.5 μg/ml) and CPT-11 (20 μg/ml) for 24 h. Subsequently, 150 μl of MTT solution (5 mg/ml) were added to each well followed by incubation for 4 h at 37˚C. Following the removal of the MTT solution, the cells were dissolved with DMSO and the absorbance was measured at 490 nm on a microplate reader (as above).

Flow cytometric detection of apoptotic cells by propidium iodide staining. The apoptosis of the IEC-6 cells was determined using the Annexin V-FITC apoptosis detection method. According the result of the protective effect of curcumin, IEC-6 cells were treated with or without 2.5 μg/ml curcumin in the presence of 20 μg/ml CPT-11 for 24 h. Following treatment for 24 h, the cells were harvested with 0.25% trypsin without EDTA, washed with cold PBS twice, and then resuspended in 400 μl binding buffer at density of 1×10^6 cells/ml. Separately, 5 μl of Annexin V-FITC and 5 μl of PI were added to the cell suspension on ice for 10 min. The apoptosis of the IEC-6 cells was assayed using a BD FACSCalibur flow cytometer (FACSCalibur cytometer, BD Biosciences, San Jose, CA, USA) for 1 h. Approximately 10,00 cells were analyzed per sample.

Flow cytometric detection of mitochondrial membrane potential. The mitochondrial membrane potential was analyzed using JC-1 dye. IEC-6 cells were treated with or without 2.5 μg/ml curcumin in the presence of 20 μg/ml CPT-11 for 24 h. Following treatment for 24 h, both floating and adherent IEC-6 cells were harvested by 0.25% trypsin without EDTA and washed twice with cold PBS. The cells were then resuspended in JC-1 staining solution and incubated at 37˚C for 25 min in the dark. The cells were then washed with PBS twice, resuspended in 0.5 ml PBS and analyzed by a BD FACSCalibur flow cytometer for 1 h. Approximately 10,000 cells were analyzed per sample.

Flow cytometric detection of reactive oxygen species (ROS). IEC-6 cells were treated with or without 2.5 μg/ml curcumin in the presence of 20 μg/ml CPT-11 for 24 h. Following treatment for 24 h, the IEC-6 cells were harvested using 0.25% trypsin

without EDTA and washed with cold PBS twice, followed by incubation with 10 μmol/l DCHF-DA for 25 min in the dark for at 37˚C. Follwoing incubation with DCHF-DA, the cells were washed with cold PBS twice, resuspended in 0.5 ml PBS and analyzed by a BD FACSCalibur flow cytometer for 1 h. Approximately 10,000 cells were analyzed for per sample.

Immunofluorescence staining. IEC-6 cells were treated with or without 2.5 μg/ml curcumin in the presence of 20 μg/ml CPT-11 for 24 h. Following treatment for 24 h, the cells were washed with PBS and fixed with 4% paraformaldehyde for 30 min. The cells were then permeabilized with 0.1% Triton X-100 for 30 min and then blocked with 0.5% bovine serum albumin for another 30 min at room temperature. After washing with PBS, the cells were incubated at 4˚C overnight with specific primary antibodies to NF-κB (1:100; cat. no. sc-71675; Santa Cruz Biotechnology, Santa Cruz, CA, USA). Afterwards, the cells were washed with PBS again and incubated in DyLight 488 affiniPure goat anti-rabbit IgG (1:500; cat. no. E032220; EarthOx Life Sciences, Millbrae, CA, USA) for 1 h in the dark at room temperature. Finally, the resulting cells were stained with DAPI (Beyotime Institute of Biotechnology). The images were visualized and captured at (x400 magnification) with an Olympus microscope.

Western blot analysis. RIPA lysis buffer was added to the intestinal tissues or IEC-6 cells for protein extraction. Following high-speed centrifugation (12,000 rpm for 15 min at 4˚C), the supernatant was collected and the protein concentration was determined using a BCA protein assay kit (Beyotime Institute of Biotechnology). The protein suspension (30 μg) mixed with 5X loading buffer (Beyotime Institute of Biotechnology), loaded onto a sodium dodecyl sulfate-polyacrylamidegel (SDS-PAGE, 8-12%) for electrophoresis and then transferred onto 0.22 μm PVDF membranes (Millipore, Billerica, MA, USA). The membranes were blocked with 5% non-fat milk at room temperature for 1 h. The membranes were then incubated overnight at 4˚C with the following primary antibodies: Glucose-regulated protein, 78 kDa (GRP78; 1:1,000; cat. no. 1587-1-AP; Proteintech, Rosemont, IL, USA), P4HB (1:1,000), PRDX4 (1:1,000), CHOP (1:1,000; cat. no. 15204-1-AP; Proteintech), cleaved caspase-3 (1:1,000; cat. no. 9664; Cell Signaling Technology, Danvers, MA, USA), β-actin (1:1,000; cat. no. BS1002; BioWorld). After washing with TBST, the membranes were incubated with goat anti-rabbit IgG-HRP (1:1,000; cat. no. BS13278; BioWorld) at room temperature for 2 h. After washing with TBST again, the membranes with proteins were visualized using ECL Plus (Millipore) and exposed by Kodak In-vivo Imaging System FX Pro (Kodak, Tokyo, Japan). The expression levels of the proteins were analyzed using ImageJ 1.48 software (National Institutes of Health, Bethesda, MD, USA). β-actin served as an internal loading control. The results are representative of 3 independent experiments.

Statistical analysis. Statistical analyses were conducted using SPSS 19 software (IBM, New York, NY, USA). Data are expressed as the means ± standard deviation (SD). Differences between groups were evaluated by two-way ANOVA followed by Fisher's least significant difference (LSD) test. A

Table I. Effects of curcumin on the diarrhea score in mice with CPT-11-induced delayed-onset diarrhea.

Group	Diarrhea scores			
	Day 6	Day 7	Day 8	Average
Control group	0	0	0	0
Model group	2.33±0.51[a]	2.33±0.51[a]	2.50±0.55[a]	2.39±0.50[a]
Curcumin therapeutic group	1.33±0.52[b]	1.67±0.84[b]	1.33±0.52[b]	1.44±0.62[b]

Data are presented as the means ± SD, n=6 mice per group. [a]$P<0.05$ vs. the control group (CON); [b]$P<0.05$ vs. the model group (CPT-11).
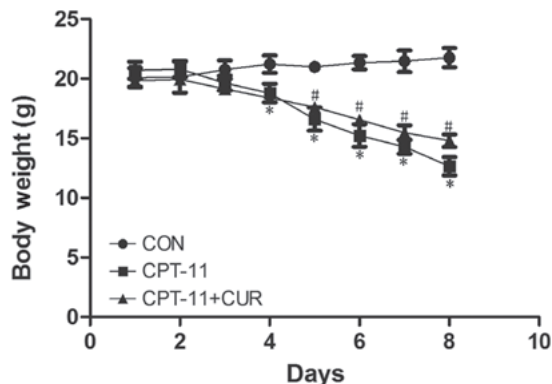

Figure 1. Effects of curcumin on the body weight of mice with CPT-11-induced delayed-onset diarrhea. Data are presented as the means ± SD, n=3 experiments. [*]$P<0.05$ vs. the control group, [#]$P<0.05$ vs. the CPT-11 group.

P-value <0.05 was considered to be a statistically significant difference.

Results

Conditions of and delayed-onset diarrhea in nude mice. The food intake and activity of the mice were significantly reduced in the diarrhea model group; symptoms of fatigue, malaise and anorexia were also apparent. The general condition of the mice in the curcumin therapeutic group had improved energy, food intake and activity and were in a better condition than the mice in the model group. The mice were weighed daily and the results of all the groups were compared. As shown in Fig. 1, the weight of the mice in the diarrhea model group was significantly lower than that of the control group ($P<0.05$). However, the weight of the mice in the curcumin therapeutic group was significantly increased compared to that of the mice in the diarrhea model group ($P<0.05$). All mice in the model group had delayed-onset diarrhea, a considerably increased stool frequency, wetter stool loose in shape, and some mice had watery stool. Stool was slightly squishy in the curcumin therapeutic group; some stool were wetter without shape; however, the frequency of diarrhea was less than that in the model group. As shown in Table I, the diarrhea scores of the curcumin therapeutic group were lower than those of the model group ($P<0.05$).

Effects of curcumin on CPT-11-induced damage to the small intestinal mucosa. H&E staining revealed a normal small intestinal mucosa structure in the control group. However, the mucosal structure was severely damaged in the CPT-11 group. Crypt structures were damaged, glands were irregularly arranged and villi were shortened or 'dropped out' with inflammatory cell infiltration. Notably, curcumin treatment significantly improve the histological structure of the intestinal mucosa (Fig. 2).

Effect of curcumin on the expression of P4HB and PRDX4 in small intestinal tissue. The molecular chaperones, P4HB and PRDX4, were detected by immunohistochemistry in the small intestinal tissue. P4HB (Fig. 3A) and PRDX4 (Fig. 3C) were mainly expressed in the cytoplasm of the small intestinal epithelial cells. As shown in Fig. 3B, the expression of P4HB in the model group was higher than that in the normal control group ($P<0.05$), and curcumin further upregulated the expression of P4HB compared with the model group ($P<0.05$). In general, as shown in Fig. 3D, the suppression of PRDX4 expression was observed following injury by CPT-11 ($P<0.05$). The CPT-11 induced suppression of PRDX4 expression was significantly reversed by treatment with curcumin ($P<0.05$). These two proteins were also examined by western blot analysis, and the results were in agreement with those obtained by immunohistochemistry (Fig. 3E-G).

Effect of curcumin and CPT-11 on IEC-6 cell viability. The effects of curcumin and CPT-11 on the viability IEC-6 cells was evaluated by MTT assay. As shown in Fig. 4A, curcumin treatment at concentrations of 0.6, 1.2 and 2.5 μg/ml exhibited no obvious cytotoxic effect on IEC-6 cells ($P>0.05$). However, at concentrations >2.5 μg/ml curcumin, dose-dependent cell death was observed ($P<0.05$). Compared with the control group, the viability of the IEC-6 cells decreased gradually with increasing concentrations of CPT-11 ($P<0.05$; Fig. 4B). IEC-6 cell viability was approximately 60% following incubation with 20 μg /ml CPT-11 for 24 h. The IEC-6 cells were also co-treated with various concentrations of curcumin (0.6, 1.2 and 2.5 μg/ml) and 20 μg/ml CPT-11 for 24 h; cell viability was increased as compared with the CPT-11 group (Fig. 4C).

Protective effects of curcumin against CPT-11-induced cytotoxicity and morphological changes. The morphological changes of the IEC-6 cells treated with or without curcumin (2.5μg/ml) in the presence of 20 μg/ml CPT-11 for 24 h were examined. Compared with the control group, the cells in the CPT-11 group were shrunken, and the size and morphology of the cells was clearly altered from a fusiform to polygonal
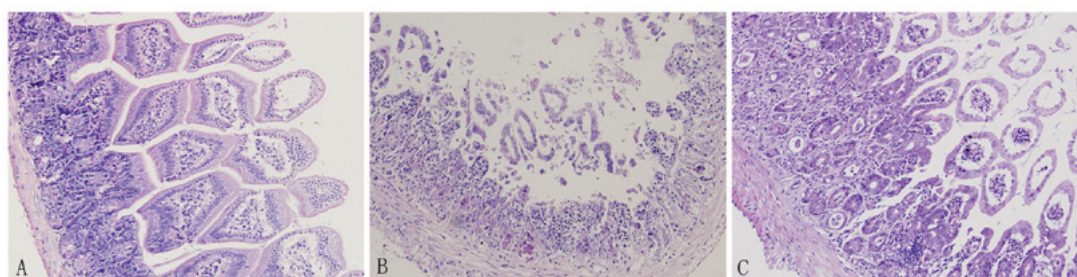
Figure 2. Histological analysis of the small intestinal mucosa. The small intestine of mice in 3 groups was analyzed by hematoxylin and eosin (H&E) staining (original magnification, x200). (A) Control group (CON); (B) model group (CPT-11); (C) curcumin therapeutic group (CPT-11 + CUR).
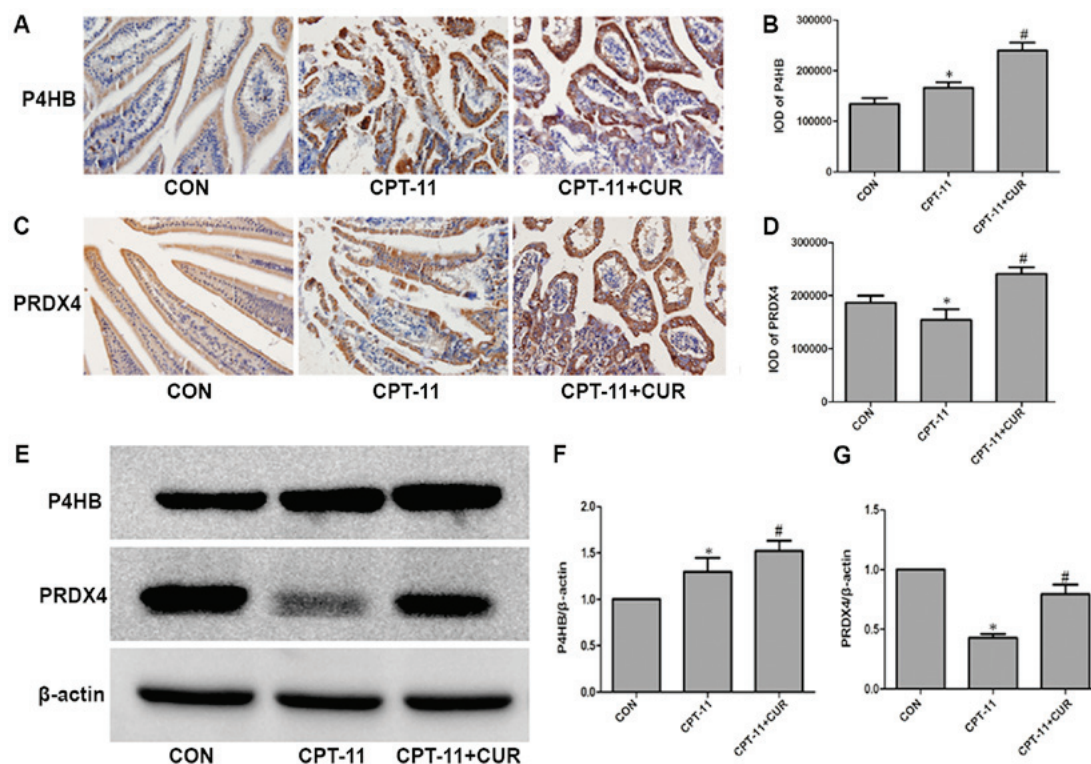

Figure 3. Effects of curcumin on the expression of P4HB and PRDX4 in mouse small intestinal tissues. (A and C) The expression of P4HB and PRDX4 was determined by immunohistochemical staining (original magnification, x400). (B and D) Integrated optical density (IOD) of P4HB and PRDX4 in small intestinal tissues were analyzed by Image-Pro Plus 6.0 software. (E) The expression levels of these two proteins were examined by western blot analysis. (F and G) Quantitative analysis of P4HB and PRDX4 expression. Data are presented as the means ± SD, n=6. $^{*}P<0.05$ vs. the control group, $^{#}P<0.05$ vs. the CPT-11 group. P4HB, prolyl 4-hydroxylase subunit beta; PRDX4, peroxiredoxin 4.

shape. As observed in the curcumin treatment group, curcumin maintained the normal morphology of the IEC-6 cells to a certain extent (Fig. 4D).

Curcumin protects the IEC-6 cells from CPT-11-induced apoptosis. Annexin V/PI staining and flow cytometry were used to detect the apoptotic rate of the IEC-6 cells. As shown in Fig. 5A, the cell apoptotic rate was significantly increased following exposure to the indicated concentration (20 μg/ml) of CPT-11 for 24 h (P<0.05). Co-treatment of the IEC-6 cells with 20 μg/ml CPT-11 and 2.5 μg/ml curcumin markedly reduced the rate of apoptosis (P<0.05). It is understood that the loss of mitochondrial membrane potential is an important event in early apoptosis. The percentage of cells in the lower right (LR) quadrant of the flow cytometric scatter plot represent the rate of early apoptosis. The analysis of mitochondrial membrane potential

revealed that compared with the control group, the percentage of cells in the LR quadrant was significantly increased in the CPT-11 group (P<0.05). However, the curcumin treatment group had a lower percentage of cells in the LR quadrant as compared to the CPT-11 group (P<0.05; Fig. 5B). The data from western blot analysis revealed that following exposure to 20 μg/ml CPT-11 for 24 h, cleaved caspase-3 expression significantly increased compared to the control group (P<0.05). Co-treatment with 2.5 μg/ml curcumin resulted in a significant decrease in CPT-11-induced cleaved caspase-3 expression (P<0.05; Fig. 5C). These results indicated that curcumin inhibited the apoptosis of the IEC-6 cells induced by CPT-11.

Protective effects of curcumin on CPT-11-induced ROS generation. As shown in Fig. 6, 20 μg/ml CPT-11 caused ROS levels to increase compared to the control group (P<0.05).
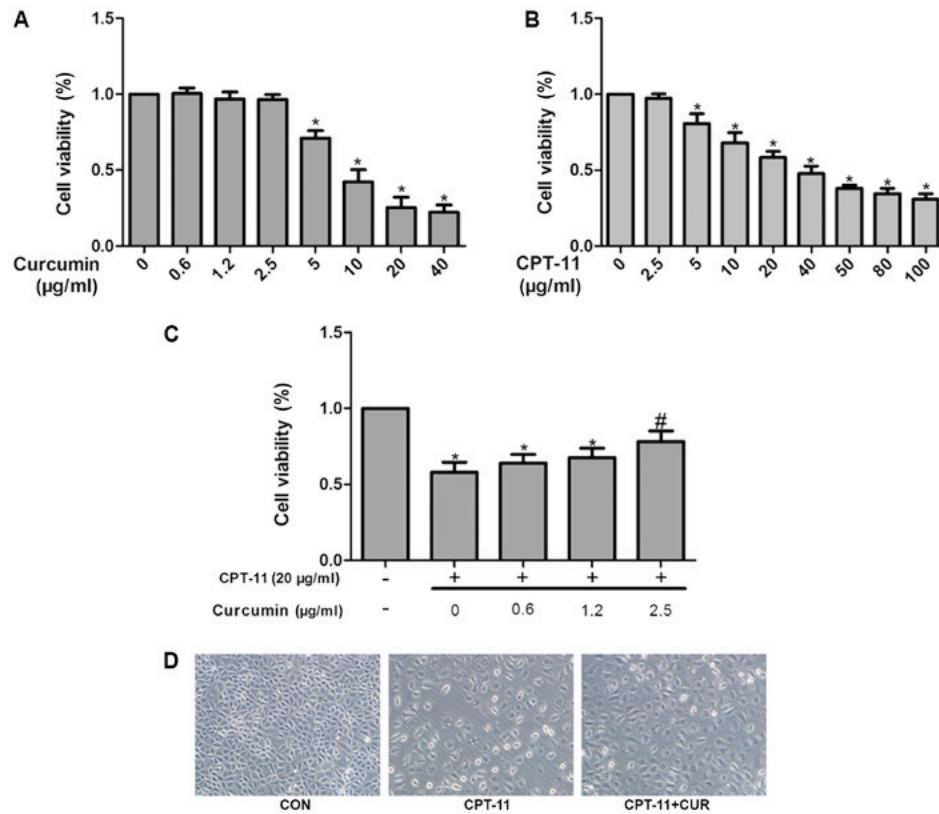
Figure 4. Effects of curcumin and CPT-11 on IEC-6 cell viability. (A) Viability of IEC-6 cells following treatment with various concentrations of curcumin, as measured by MTT assay. (B) Viability of IEC-6 cells following treatment with various concentrations of CPT-11, as measured by MTT assay. (C) IEC-6 cells were treated with 20 μg/ml CPT-11 with or without various of concentrations of curcumin (0.6, 1.2 and 2.5 μg/ml) for 24 h. Data are presented as the means ± SD, n=3 experiments. *P<0.05 vs. the control group, #P<0.05 vs. the CPT-11 (20 μg/ml) group. (D) The effect of curcumin on CPT-11-induced cell morphological changes (original magnification, x200).
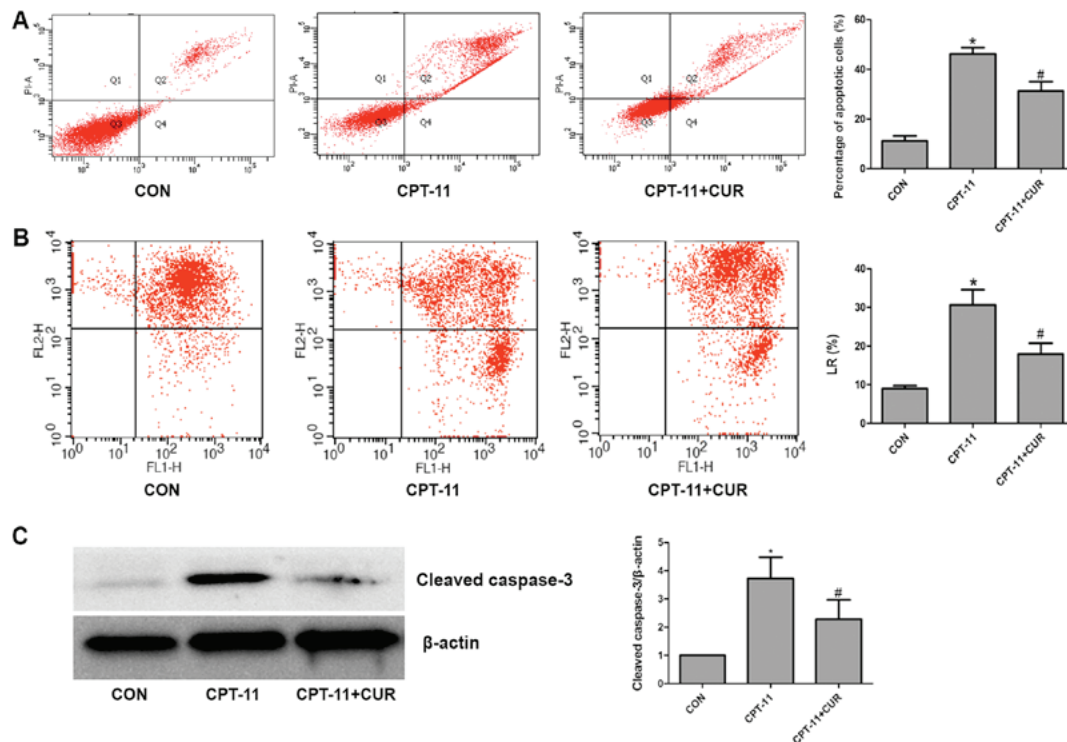

Figure 5. Curcumin inhibits CPT-11-induced IEC-6 cells apoptosis. (A) IEC-6 cells were treated with or without 2.5 μg/ml curcumin in the presence of 20 μg/ml CPT-11 for 24 h and apoptotic cells were detected by flow cytometry following Annexin V and PI double-staining. (B) IEC-6 cells were treated with or without 2.5 μg/ml curcumin in the presence of 20 μg/ml CPT-11 for 24 h. Mitochondrial membrane potential was measured by flow cytometry using JC-1 dye. (C) IEC-6 cells were treated with 20 μg/ml CPT-11 with or without 2.5 μg/ml curcumin for 24 h and the expression of cleaved caspase-3 was detected by western blot analysis. Data are presented as the means ± SD, n=3 experiments. *P<0.05 vs. the control group, #P<0.05 vs. the CPT-11 group.
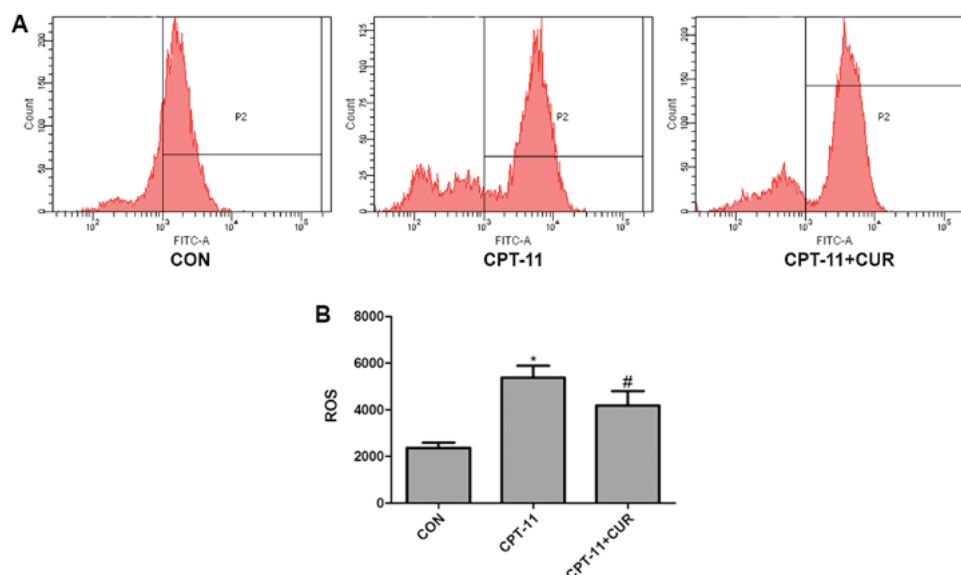
Figure 6. Curcumin reduces CPT-11-induced reactive oxygen species (ROS) production. (A) IEC-6 cells were treated with or without 2.5 µg/ml curcumin in the presence of 20 µg/ml CPT-11 for 24 h. Intracellular ROS was determined by flow cytometry. (B) Quantitative analysis of ROS. Data are presented as the means ± SD, n=3 experiments. *P<0.05 vs. the control group, #P<0.05 vs. the CPT-11 group.
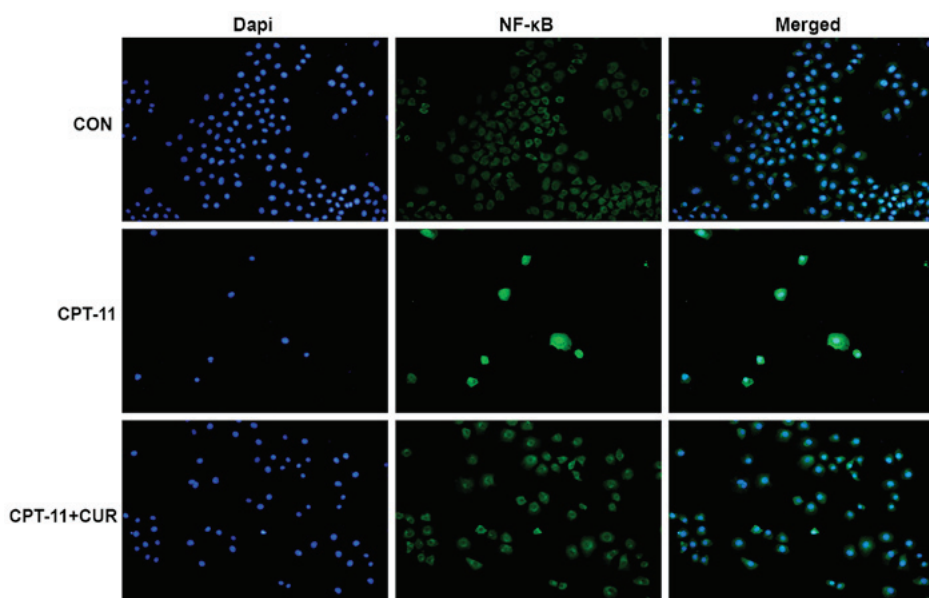

Figure 7. Effects of curcumin on the blockage of nuclear factor (NF)-κB translocation into the nucleus (original magnification, x200). Immunofluorescence staining visualizes the expression and distribution of NF-κB p65 in response to CPT-11 with or without curcumin treatment. Cell nuclei were stained with DAPI and NF-κB p65 was stained with corresponding antibody. In control cells and cells treated with CPT-11 + CUR, NF-κB was detected in the cytoplasm. In cells treated with CPT-11, the nuclear translocation of NF-κB was evident.

However, treatment with 2.5 µg/ml curcumin suppressed the generation of ROS induced by CPT-11 (P<0.05). These findings suggest that curcumin reduces ROS levels which are indcued by CPT-11.

Curcumin inhibits the CPT-11-induced nuclear translocation of NF-κB. Normally, NF-κB is a dimer mainly composed of NF-κB p65 and NF-κB p50 subunits and is maintained in an inactive state in the cytoplasm. When cells are stimulated by internal or external factors, such as lipopolysaccharide (LPS), TNF-α or CPT-11, NF-κB p65 is released from the NF-κB transcription complex and translocates to the nucleus in order to

activate a series of gene transcription (12,15-17). In this study, the nuclear translocation of NF-κB p65 in the IEC-6 cells was analyzed by immunofluorescence staining. The results revealed that NF-κB p65 was expressed in the cytoplasm of the untreated IEC-6 cells, whereas CPT-11 induced the nuclear translocation of NF-κB p65. Curcumin significantly reduced the NF-κB p65 nuclear translocation induced by CPT-11 in the IEC-6 cells (Fig. 7).

Effect of curcumin on ER stress-associated proteins. To determine whether the CPT-11-induced apoptosis of IEC-6 cells occurs through ER stress the effect of curcumin on ER
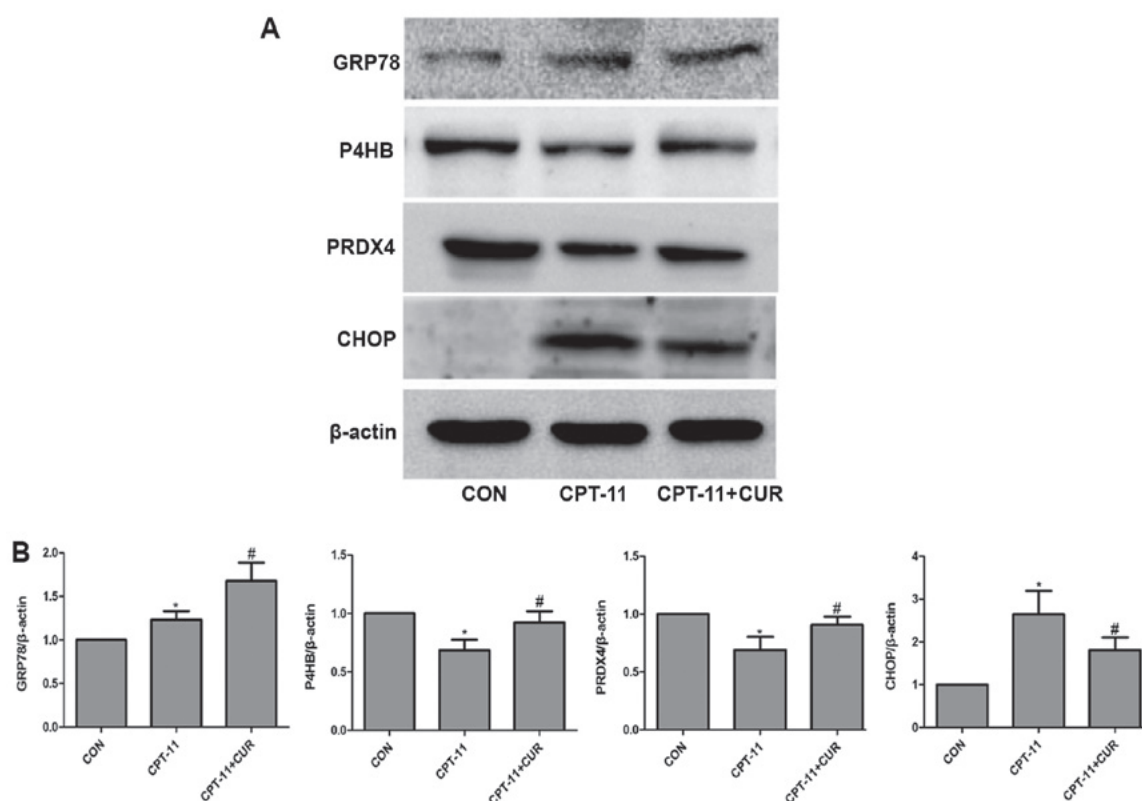
Figure 8. Effects of curcumin on endoplasmic reticulum (ER) stress-induced changes in GRP78, P4HB, PRDX4 and CHOP expression. (A) IEC-6 cells were treated with or without 2.5 μg/ml curcumin in the presence of 20 μg/ml CPT-11 for 24 h and the expression of GRP78, P4HB, PRDX4 and CHOP was determined by western blot analysis. (B) Quantitative analysis of the relative protein levels of GRP78, P4HB, PRDX4 and CHOP. Data are presented as the means ± SD, n=3 experiments. *P<0.05 vs. the control group, $^#$P<0.05 vs. the CPT-11 group. GRP78, glucose-regulated protein, 78 kDa; P4HB, prolyl 4-hydroxylase subunit beta; PRDX4, peroxiredoxin 4.

stress-induced cell death, the expression levels of the ER stress-associated proteins, GRP78, P4HB, PRDX4 and CHOP, were examined by western blot analysis. As expected, the level of GRP78 in the CPT-11 group was upregulated compared to the control group (P<0.05), and compared with the CPT-11 group, curcumin caused a robust enhancement of GRP78 expression (P<0.05). In addition, the group exposed to CPT-11 exhibited a significant reduction in the expression levels of P4HB and PRDX4 (P<0.05) compared with the control group. Curcumin suppressed the upregulation of these two proteins induced by CPT-11 (P<0.05). Furthermore, the expression of CHOP was also significantly increased compared with the control group (P<0.05), while curcumin markedly decreased CHOP expression (P<0.05; Fig. 8). Thus, it was demonstrated that CPT-11 induces injury to and the apoptosis of IEC-6 cells through the activation of ER stress, and ER stress is significantly suppressed by curcumin treatment.

Discussion

Curcumin has poor systemic availability due to its low aqueous solubility, efficient first-pass effect and a certain degree of intestinal metabolism when administered via the oral route. However, in this study, we demonstrated that curcumin exerted a protective effect on CPT-11 induced intestinal mucosal injury both *in vivo* and *in vitro*. *In vivo*, we found that the general and diarrheal conditions of the nude mice in the curcumin therapeutic group were better than those of the mice

in the model group. With light microscopy we also observed that curcumin improved intestinal mucosal injury caused by CPT-11. Moreover, *in vitro*, treatment with 2.5 μg/ml curcumin exhibited no cytotoxicity and effectively improved the viability of the IEC-6 cells treated with CPT-11 at 20 μg/ml for 24 h. In addition, the data from IEC-6 cell morphological observation, cell apoptosis assay, mitochondrial membrane potential assay and apoptosis protein cleaved caspase-3 detection demonstrated that curcumin reduced CPT-11-induced apoptosis, which indicates that this molecule may exert a protective effect against certain chemotherapeutic drugs.

Currently, CPT-11-induced intestinal mucosal injury mainly manifests as late-onset diarrhea; however, the mechanisms of the pathogenesis of late-onset diarrhea remain unclear. It is accepted that following absorption into the body, CPT-11 is metabolized by enzymes, such as carboxylesterase (CES), cytochrome P450 (CYP) and intestinal β glucose polygalacturonase (β-glucuronidase) and is changed into the active metabolite, SN-38, which directly damages intestinal mucosa cells (4). In addition, CPT-11-induced intestinal mucosal injury can cause a variety of signals, such as the activation of NF-κB pathway, the upregulated expression of the inflammation related factors, COX-2, PGE2 and TAX2, and the promotion of the inflammatory factors, TNF-α and IL-1β, resulting in inflammation within the intestines and damage to the intestinal mucosal barrier function (5). Moreover, the UGT1A1 gene polymorphism (6), intestinal epithelial cell tight junction protein destruction (7) and bacteria group translocation (8)

might be possible mechanisms of CPT-11 induced diarrhea. In this study, following CPT-11 treatment at 20 μg/ml for 24 h, NF-κB in the IEC-6 cells was localized to the nucleus from the cytoplasm. In addition, the level of ROS was significantly increased, and the results of western blot analysis revealed that CPT-11 upregulated the expression of the ER stress-related marker proteins, GRP78 and CHOP. Thus, the mechanisms of CPT-11-induced intestinal mucosa injury are not only related with NF-κB activation, but also with oxidative and ER stress.

As a traditional Chinese medicine, curcumin has many characteristics, such as an abundant source, low toxicity, multiple molecular targets and is well-tolerated. It also has a wide range of pharmacological effects, including anti-inflammatory, antioxidant, anti-fibrotic and anti-tumor activity (9-11). NF-κB is a nuclear transcription factor, involved in various inflammatory responses, cell stress, cell transformation, tumor invasion and drug resistance (15). Normally, NF-κB is a dimer mainly composed of NF-κB p65 and NF-κB p50 subunits and is maintained in an inactive state in the cytoplasm. When the cells are stimulated by internal and external factors, such as LPS, TNF-α or CPT-11, NF-κB p65 is released from the NF-κB transcription complex and translocates to the nucleus in order to activate a series of gene transcription and expression including IL-2, IL-6, ICAM-1, E-selectin among others (16,17). This is the classical NF-κB activation pathway.

A large number of studies have proven that curcumin inhibits the NF-κB activation. As demonstrated by Song *et al* (12), curcumin exerted a protective effect on MTX-induced rat enteritis, and the underlying mechanism involved the inhibition of the activation of NF-κB in intestinal mucosal cells and the regulation of the production of inflammatory factors and cytokines by curcumin, probably via the NF-κB signaling pathway. In human articular cartilage cells, has been shown to curcumin inhibit the activation of NF-κB induced by IL-1β (18). Jian *et al* (19) also found that curcumin inhibited NF-κB activation in a colitis model induced by trinitrobenzene sulfonic acid. In this study, CPT-11 induced the nuclear translocation of NF-κB p65 in IEC-6 cells, and curcumin significantly reduced NF-κB p65 nuclear translocation induced by CPT-11 in IEC-6 cells. It was thus suggested that the inhibitory effects of curcumin against the production of inflammatory factors and cytokines probably occurred via the NF-κB signaling pathway.

In addition, some studies have indicated that an increase in ROS generation is an important factor in intestinal mucosal injury. As an important factor, SOD can effectively scavenge oxygen free radical ROS and can inhibit lipid peroxidation, so as to reduce the level of MDA, thus playing a role as an antioxidant (20). *In vitro*, wheat peptide administration may be an effective tool for protecting small intestinal tissue against non-steroidal anti-inflammatory drug (NSAID)-induced small intestinal damage and oxidative stress by suppressing NF-κB activation and regulating the expression levels of SOD, glutathione peroxidase (GPx) and MDA (21).

DNA damage is the one cell killing mechanisms of CPT-11. Kang *et al* (22) indicated that DNA damage induces ROS generation. Therefore, we hypothesized that CPT-11 may induce DNA damage in IEC-6 cells and result in increasing intracellular ROS levels and NF-κB activation, disrupting the intestinal redox balance, and causing intestinal mucosal

injury, as well as inducing cell apoptosis. Antioxidant activity, the scavenging oxygen free radicals, is an important pharmacological effect of curcumin. In a diabetic rat model of gastric light paralysis, curcumin was shown to improve gastric emptying symptoms, and this mechanism may block the generation of oxidative stress, and inhibit the signal transduction of NF-κB (23). Arafa *et al* (13) demonstrated that curcumin increased intestinal SOD, GSH and GST, and downregulated MDA levels in a model of ulcerative colitis models induced by DSS. *In vitro*, in this study, curcumin inhibited the upregulation of ROS induced by CPT-11 in IEC-6 cells. Thus, curcumin can effectively scavenge oxygen free radicals and can counteract oxidative damage in the intestinal mucosa induced by CPT-11.

Moreover, we found that ER stress participated in the pathogenesis of CPT-11-induced intestinal mucosal injury. The ER is the main site of protein synthesis, lipid production and Ca^{2+} storage in eukaryotic cells. When the cells are in a low sugar, hypoxic and acidosis microenvironment, or if there is a calcium ion, or redox imbalance, unfolded or misfolded proteins will gather in the endoplasmic reticulum causing endoplasmic reticulum stress and activation of the unfolded protein response (UPR) (24).

The unfolded protein response is mainly mediated by the activation of three transmembrane proteins, inositol-requiring enzyme 1 (IRE1), protein kinase R-like endoplasmic reticulum kinase (PERK) and activating transcription factor 6 (ATF6). Under normal resting conditions, these transmembrane proteins are bound to the ER stress marker protein, GRP78, in an inactive form. When ER stress occurs, GRP78 dissociates from the three membrane proteins and plays the role of a molecular chaperone, inducing the synthesis of other molecular chaperones such as P4HB and PRDX4, and promoting the correct refolding of protein in order to maintain the endoplasmic reticulum homeostasis (24-26). However, when the pressure of ER stress is too strong or prolonged, it leads to insufficient endoplasmic reticulum homeostasis, CHOP/GADD153 expression, JNK activation and caspase-12 expression will be induced, eventually leading to cell apoptosis (27). In addition, Bcl-2 and Bax are two classic proteins in the apoptotic pathway. They are mutually validated and have a clear persuasion in terms of apoptosis. and these two proteins will be the direction of our future research. From what has been mentioned above, the inhibition of ER stress can play a protective role in cells and tissues.

Kim *et al* (28) indicated that NELL2 upregulated GRP78 and downregulated CHOP expression by the regulation of the ERK signaling pathway, thereby inhibiting the apoptosis of COS-7 cells induced by ER stress. Similarly, Xu *et al* (29) demonstrated that GSP upregulated GRP78 and downregulated the expression of CHOP, which alleviates endoplasmic reticulum stress caused by hepatic ischemia reperfusion in rats. It has also been reported that curcumin potently inhibits ER stress. Afrin *et al* (30) found that streptozotocin (STZ) induced liver injury in diabetic rats via ER stress and that curcumin alleviated liver ER stress by regulating the expression of GRP78, ASK, IRE1 and CHOP proteins. Curcumin has also been shown to suppress ER stress and oxidative stress in mouse hippocampal cells induced by CoCl$_2$ (31).

In this study, following treatment with CPT-11 for 24 h, the expression of GRP78 was markedly increased, resulting in ER stress in IEC-6 cells. The expression levels of GRP78, P4HB and PRDX4 were increased further in the curcumin protection group compared to the CPT-11 group. As molecular chaperones, these proteins exert a certain protective effect by helping to correctly fold unfolded or misfolded proteins and maintaining ER homeostasis. CHOP, as a specific protein in the ER stress pathway, mediates apoptosis by regulating the mitochondrial apoptosis pathway or the expression of death receptors (24,25,27). Therefore, it follows that the CHOP expression level directly reflects the strength of ER stress. In this study, the expression of CHOP in CPT-11 group was also increased significantly compared to the control group. It is therefore clear that curcumin markedly reduces the relative amounts of CHOP. These results indicate that curcumin can protect intestinal mucosa cells by improving or mitigating ER stress induced by CPT-11.

In conclusion, the findings of this study demonstrate that curcumin exets a protective effect against CPT-11-induced intestinal mucosal injury mediated by the inhibition of NF-κB activation, oxidative stress and ER stress, induced by CPT-11. Recent studies have demonstrated that NF-κB activation, oxidative stress and ER stress are interrelated biological process that commonly regulate signal transduction pathways in cells, and participate in the development of human physiological changes and diseases. However, the association among these three has not yet been clarified (32,33). It was thus concluded that the protective effects of curcumin is mediated by suppressing the NF-κB activation, oxidative stress and ER stress. However, how to improve the bioavailability of curcumin, and the specific signaling pathways where curcumin plays a role and the association between these three physiological processes in this manuscript will be the focus of our research in the future.

Availability of data and materials

The datasets used and/or analyzed during the current study are available from the corresponding author on reasonable request.

Authors' contributions

XY, ZL and MO conceived and designed the experiments. ZL and WZ performed the experiments and acquired data. DZ, YL and JW provided the methodology, analyzed and interpreted the data. ZL and WZ drafted the manuscript. XY and MO directed the writing of the manuscript. ZL revised the manuscript. All authors have read and approved the final manuscript.

Ethics approval and consent to participate

This study was approved by the Institutional Animal Care and Use Committee of Southern Medical University.

Patient consent for publication

Not applicable.

Competing interests

The authors declare that they have no competing interests.

References

1. Tanizawa A, Fujimori A, Fujimori Y and Pommier Y: Comparison of topoisomerase I inhibition, DNA damage, and cytotoxicity of camptothecin derivatives presently in clinical trials. J Natl Cancer Inst 86: 836-842, 1994.
2. Bleiberg H and Cvitkovic E: Characterisation and clinical management of CPT-11 (irinotecan)-induced adverse events: The European perspective. Eur J Cancer 32A (Suppl 3): S18-S23, 1996.
3. Benson AB III, Ajani JA, Catalano RB, Engelking C, Kornblau SM, Martenson JA Jr, McCallum R, Mitchell EP, O'Dorisio TM, Vokes EE, *et al*: Recommended guidelines for the treatment of cancer treatment-induced diarrhea. J Clin Oncol 22: 2918-2926, 2004.
4. Sanghani SP, Quinney SK, Fredenburg TB, Davis WI, Murry DJ and Bosron WF: Hydrolysis of irinotecan and its oxidative metabolites, 7-ethyl-10-[4-N-(5-aminopentanoic acid)-1-piperidino] carbonyloxycamptothecin and 7-ethyl-10-[4-(1-piperidino)-1-a mino]-carbonyloxycamptothecin, by human carboxylesterases CES1A1, CES2, and a newly expressed carboxylesterase isoenzyme, CES3. Drug Metab Dispos 32: 505-511, 2004.
5. Swami U, Goel S and Mani S: Therapeutic targeting of CPT-11 induced diarrhea: A case for prophylaxis. Curr Drug Targets 14: 777-797, 2013.
6. Xu JM, Wang Y, Ge FJ, Lin L, Liu ZY and Sharma MR: Severe irinotecan-induced toxicity in a patient with UGT1A1 28 and UGT1A1 6 polymorphisms. World J Gastroenterol 19: 3899-3903, 2013.
7. Nakao T, Kurita N, Komatsu M, Yoshikawa K, Iwata T, Utusnomiya T and Shimada M: Irinotecan injures tight junction and causes bacterial translocation in rat. J Surg Res 173: 341-347, 2012.
8. Lin XB, Farhangfar A, Valcheva R, Sawyer MB, Dieleman L, Schieber A, Gänzle MG and Baracos V: The role of intestinal microbiota in development of irinotecan toxicity and in toxicity reduction through dietary fibres in rats. PLoS One 9: e83644, 2014.
9. Aggarwal BB, Gupta SC and Sung B: Curcumin: An orally bioavailable blocker of TNF and other pro-inflammatory biomarkers. Br J Pharmacol 169: 1672-1692, 2013.
10. Woo JM, Shin DY, Lee SJ, Joe Y, Zheng M, Yim JH, Callaway Z and Chung HT: Curcumin protects retinal pigment epithelial cells against oxidative stress via induction of heme oxygenase-1 expression and reduction of reactive oxygen. Mol Vis 18: 901-908, 2012.
11. Rahmani AH, Al Zohairy MA, Aly SM and Khan MA: Curcumin: A potential candidate in prevention of cancer via modulation of molecular pathways. BioMed Res Int 2014: 761608, 2014.
12. Song WB, Wang YY, Meng FS, Zhang QH, Zeng JY, Xiao LP, Yu XP, Peng DD, Su L, Xiao B, *et al*: Curcumin protects intestinal mucosal barrier function of rat enteritis via activation of MKP-1 and attenuation of p38 and NF-κB activation. PLoS One 5: e12969, 2010.
13. Arafa HM, Hemeida RA, El-Bahrawy AI and Hamada FM: Prophylactic role of curcumin in dextran sulfate sodium (DSS)-induced ulcerative colitis murine model. Food Chem Toxicol 47: 1311-1317, 2009.
14. Zhu DJ, Chen XW, Wang JZ, Ju YL, Ou Yang MZ and Zhang WJ: Proteomic analysis identifies proteins associated with curcumin-enhancing efficacy of irinotecan-induced apoptosis of colorectal cancer LOVO cell. Int J Clin Exp Pathol 7: 1-15, 2013.

15. Hoesel B and Schmid JA: The complexity of NF-κB signaling in inflammation and cancer. Mol Cancer 12: 86, 2013.
16. Meng Z, Yan C, Deng Q, Gao DF and Niu XL: Curcumin inhibits LPS-induced inflammation in rat vascular smooth muscle cells in vitro via ROS-relative TLR4-MAPK/NF-κB pathways. Acta Pharmacol Sin 34: 901-911, 2013.
17. Logan RM, Gibson RJ, Bowen JM, Stringer AM, Sonis ST and Keefe DM: Characterisation of mucosal changes in the alimentary tract following administration of irinotecan: Implications for the pathobiology of mucositis. Cancer Chemother Pharmacol 62: 33-41, 2008.
18. Csaki C, Mobasheri A and Shakibaei M: Synergistic chondroprotective effects of curcumin and resveratrol in human articular chondrocytes: Inhibition of IL-1beta-induced NF-kappaB-mediated inflammation and apoptosis. Arthritis Res Ther 11: R165, 2009.
19. Jian YT, Mai GF, Wang JD, Zhang YL, Luo RC and Fang YX: Preventive and therapeutic effects of NF-kappaB inhibitor curcumin in rats colitis induced by trinitrobenzene sulfonic acid. World J Gastroenterol 11: 1747-1752, 2005.
20. Wei Q, Ren X, Jiang Y, Jin H, Liu N and Li J: Advanced glycation end products accelerate rat vascular calcification through RAGE/oxidative stress. BMC Cardiovasc Disord 13: 13, 2013.
21. Yin H, Pan X, Song Z, Wang S, Yang L and Sun G: Protective effect of wheat peptides against indomethacin-induced oxidative stress in IEC-6 cells. Nutrients 6: 564-574, 2014.
22. Kang MA, So EY, Simons AL, Spitz DR and Ouchi T: DNA damage induces reactive oxygen species generation through the H2AX-Nox1/Rac1 pathway. Cell Death Dis 3: e249, 2012.
23. Jin QH, Shen HX, Wang H, Shou QY and Liu Q: Curcumin improves expression of SCF/c-kit through attenuating oxidative stress and NF-κB activation in gastric tissues of diabetic gastroparesis rats. Diabetol Metab Syndr 5: 12, 2013.
24. Latham KE: Endoplasmic reticulum stress signaling in mammalian oocytes and embryos: Life in balance. Int Rev Cell Mol Biol 316: 227-265, 2015.
25. Schönthal AH: Endoplasmic reticulum stress: Its role in disease and novel prospects for therapy. Scientifica (Cairo) 2012: 857516, 2012.
26. Bravo R, Parra V, Gatica D, Rodriguez AE, Torrealba N, Paredes F, Wang ZV, Zorzano A, Hill JA, Jaimovich E, et al: Endoplasmic reticulum and the unfolded protein response: Dynamics and metabolic integration. Int Rev Cell Mol Biol 301: 215-290, 2013.
27. Liu MQ, Chen Z and Chen LX: Endoplasmic reticulum stress: A novel mechanism and therapeutic target for cardiovascular diseases. Acta Pharmacol Sin 37: 425-443, 2016.
28. Kim DY, Kim HR, Kim KK, Park JW and Lee BJ: NELL2 function in the protection of cells against endoplasmic reticulum stress. Mol Cells 38: 145-150, 2015.
29. Xu ZC, Yin J, Zhou B, Liu YT, Yu Y and Li GQ: Grape seed proanthocyanidin protects liver against ischemia/reperfusion injury by attenuating endoplasmic reticulum stress. World J Gastroenterol 21: 7468-7477, 2015.
30. Afrin R, Arumugam S, Soetikno V, Thandavarayan RA, Pitchaimani V, Karuppagounder V, Sreedhar R, Harima M, Suzuki H, Miyashita S, et al: Curcumin ameliorates streptozotocin-induced liver damage through modulation of endoplasmic reticulum stress-mediated apoptosis in diabetic rats. Free Radic Res 49: 279-289, 2015.
31. Chhunchha B, Fatma N, Kubo E, Rai P, Singh SP and Singh DP: Curcumin abates hypoxia-induced oxidative stress based-ER stress-mediated cell death in mouse hippocampal cells (HT22) by controlling Prdx6 and NF-κB regulation. Am J Physiol Cell Physiol 304: C636-C655, 2013.
32. Bhandary B, Marahatta A, Kim HR and Chae HJ: An involvement of oxidative stress in endoplasmic reticulum stress and its associated diseases. Int J Mol Sci 14: 434-456, 2012.
33. Chaudhari N, Talwar P, Parimisetty A, Lefebvre d'Hellencourt C and Ravanan P: A molecular web: Endoplasmic reticulum stress, inflammation, and oxidative stress. Front Cell Neurosci 8: 213, 2014.